Current Biology *16*, 939–944, May 9, 2006 ©2006 Elsevier Ltd All rights reserved DOI 10.1016/j.cub.2006.03.065

Report

Regulation of *AUXIN RESPONSE FACTOR3* by *TAS3* ta-siRNA Affects Developmental Timing and Patterning in *Arabidopsis*

Noah Fahlgren,[1,2] Taiowa A. Montgomery,[1,2] Miya D. Howell,[1,2] Edwards Allen,[1,3] Sarah K. Dvorak,[1] Amanda L. Alexander,[1] and James C. Carrington[1,*]
[1] Center for Genome Research and Biocomputing and Department of Botany and Plant Pathology
Oregon State University
Corvallis, Oregon 97330

Summary

MicroRNAs (miRNAs) and *trans*-acting siRNAs (ta-siRNAs) in plants form through distinct pathways, although they function as negative regulators of mRNA targets by similar mechanisms [1–7]. Three ta-siRNA gene families (*TAS1*, *TAS2*, and *TAS3*) are known in *Arabidopsis thaliana*. Biogenesis of *TAS3* ta-siRNAs, which target mRNAs encoding several AUXIN RESPONSE FACTORs (including ARF3/ETTIN and ARF4 [1, 8]) involves miR390-guided processing of primary transcripts, conversion of a precursor to dsRNA through RNA-DEPENDENT RNA POLYMERASE6 (RDR6) activity, and sequential DICER-LIKE4 (DCL4)-mediated cleavage events. We show that the juvenile-to-adult phase transition is normally suppressed by *TAS3* ta-siRNAs, in an ARGONAUTE7-dependent manner, through negative regulation of *ARF3* mRNA. Expression of a nontargeted *ARF3* mutant (*ARF3mut*) in a wild-type background reproduced the phase-change phenotypes detected in *rdr6-15* and *dcl4-2* mutants, which lose all ta-siRNAs. Expression of either *ARF3* or *ARF3mut* in *rdr6-15* plants, in which both endogenous and transgenic copies of *ARF3* were derepressed, resulted in further acceleration of phase change and severe morphological and patterning defects of leaves and floral organs. In light of the functions of *ARF3* and *ARF4* in organ asymmetry, these data reveal multiple roles for *TAS3* ta-siRNA-mediated regulation of *ARF* genes in developmental timing and patterning.

Results/Discussion

ZIP (*AGO7*) Is Required for the Accumulation of *TAS3* ta-siRNAs

Loss-of-function mutations affecting ta-siRNA biogenesis factors lead to accelerated juvenile-to-adult phase change in *Arabidopsis* [4]. Characteristics associated with the adult stage, such as downward-curled leaves, abaxial trichomes, and elongated leaves, appear sooner in *rdr6-15* and *dcl4-2* mutants compared to wild-type (Col-0) plants [4, 6, 9, 10]. Similar phenotypes are associated with *zip-1*, which has a defect in AGO7 [9] (Figure 1A). RNA-blot assays for *TAS1*, *TAS2*, and *TAS3* ta-siRNAs were done with triplicate samples from wild-type Col-0, *zip-1*, and *rdr6-15* plants to test the hypothesis that *ZIP* has a specific role in ta-siRNA function. In addition, four miRNAs (miR171, miR173, miR390, and miR391) were analyzed. *ZIP* was not required for any of the miRNAs tested, although there were quantitative effects for each (Figure 1C). Similarly, *ZIP* was not required for *TAS1* (ta-siR255) or *TAS2* (ta-siR1511) ta-siRNAs (Figure 1C). In contrast, *TAS3*-derived ta-siRNAs (Figure 1B) required *ZIP*, because these were lost in the *zip-1* mutant (Figure 1C). The unique requirement of *TAS3* ta-siRNAs for *ZIP* differed from the dependence of all ta-siRNAs on *RDR6* (Figure 1C).

With the assumption that AGO7 is similar to AGO1 [11] and AGO4 [12, 13], small RNAs that function in association with AGO7 are generally predicted to be destabilized and accumulate to low or nondetectable levels in *zip-1* mutant plants. Given that *TAS3* ta-siRNAs are lost in *zip-1* plants, we predict that AGO7 functions with *TAS3*-derived ta-siRNAs. It is also possible that AGO7 functions with miR390 during *TAS3* transcript processing, although the elevated level of miR390 in *zip-1* plants (Figure 1C) argues against this idea. Because a *TAS1* ta-siRNA was shown to associate with AGO1 [14], we conclude that distinct ta-siRNAs are functionally associated with different AGO proteins in effector complexes.

Nontargeted *ARF3mut* Triggers Accelerated Phase Change

Given that general ta-siRNA-defective mutants (*rdr6-15* and *dcl4-2*) and *zip-1* exhibit accelerated vegetative phase-change phenotypes [2, 4, 6, 9], and that *ZIP*-dependent *TAS3* ta-siRNAs are known to target *ARF3* and *ARF4* [1], we hypothesized that the phase-change phenotypes are due to deficiencies in regulation of *ARFs* by *TAS3* ta-siRNAs. On the basis of genetic analyses, *ARF3* and *ARF4* likely have overlapping functions in leaf and floral organ patterning and cooperate with *KANADI* genes to specify abaxial cell identity [15]. Members of the ARF family generally function by interaction with auxin response elements after dissociating from inhibitory AUX/IAA proteins in the presence of auxin [16, 17]. A *TAS3* ta-siRNA-insensitive mutant of *ARF3* (*ARF3:ARF3mut*) was generated by introducing silent mutations into the "A" and "B" target sites (Figure 2A). The mutations placed each site in violation of targeting "rules" [1, 18, 19]. Both targeted *ARF3* and nontargeted *ARF3mut* were introduced with their authentic 5′ and 3′ regulatory sequences into wild-type Col-0 and *rdr6-15* mutant plants. Additionally, control Col-0 and *rdr6-15* plants were transformed with the empty cloning vector.

Relative levels of *ARF3* sequences in Col-0 and *rdr6-15* plants expressing each construct were measured by quantitative RT-PCR. As shown previously, *ARF3* transcripts accumulated to higher levels in control *rdr6-15* inflorescences relative to the *ARF3* transcript levels in Col-0 inflorescences (Figure 2B) [1, 4, 6].

*Correspondence: carrington@cgrb.oregonstate.edu
[2] These authors contributed equally to this work.
[3] Present address: Monsanto Company, Chesterfield, Missouri, 63017.

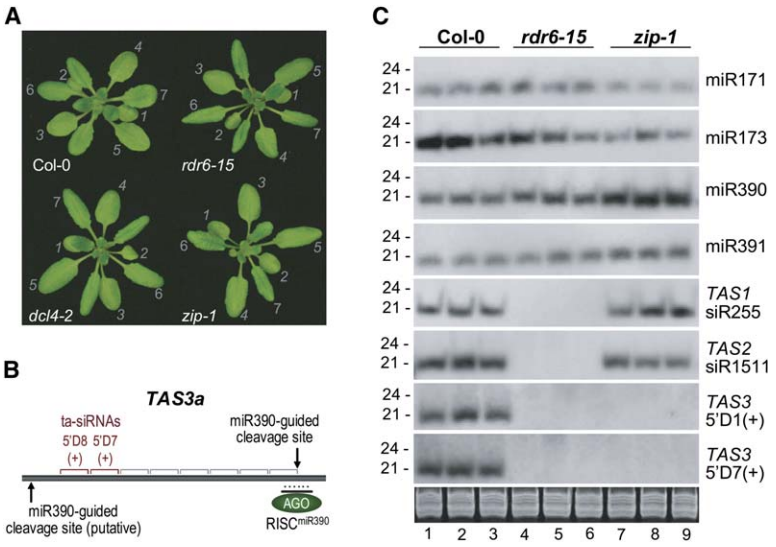

Figure 1. *trans*-Acting siRNAs and Vegetative Development

(A) Rosette phenotypes associated with *rdr6-15*, *dcl4-2*, and *zip-1*. Leaves 1–7 are indicated.

(B) Organization of the *TAS3a* transcript. The ta-siRNAs from the 5′D7(+) and 5′D8(+) positions are indicated, as are the validated and predicted miR390-guided cleavage sites.

(C) RNA-blot assays for four miRNAs (miR171, miR173, miR390, and miR391) and four ta-siRNAs [*TAS1*-siR255, *TAS2*-siR1511, *TAS3*-5′D1(+), and *TAS3*-5′D7(+)]. Three independent samples for each genotype were analyzed. Ethidium-bromide-stained 5S ribosomal and tRNAs are also shown as loading controls.

ARF3 transcript levels similar to those in *rdr6-15* plants were detected in Col-0 inflorescences expressing the targeted *ARF3* transgene and at levels above those in *rdr6-15* plants expressing the nontargeted *ARF3mut* transgene (Figure 2B). This suggests that elevated *ARF3* transcript levels detected in Col-0 plants expressing targeted *ARF3* were due to an increase in copy number, whereas the further increases in the nontargeted *ARF3mut* lines were due to higher copy number and derepression of the *ARF3mut* transcript. This was supported further by analysis of *rdr6-15* plants transformed with targeted *ARF3* and nontargeted *ARF3mut* transgenes, which both led to significantly higher transcript levels (Figure 2B). In contrast to Col-0 plants expressing the transgenes, *ARF3* transcripts in *rdr6-15* plants expressing either targeted or nontargeted transgenes accumulated to comparable levels. This was consistent with expectations, because both endogenous *ARF3* and transgene-derived *ARF3* or *ARF3mut* sequences lacked negative regulation by *TAS3* ta-siRNAs

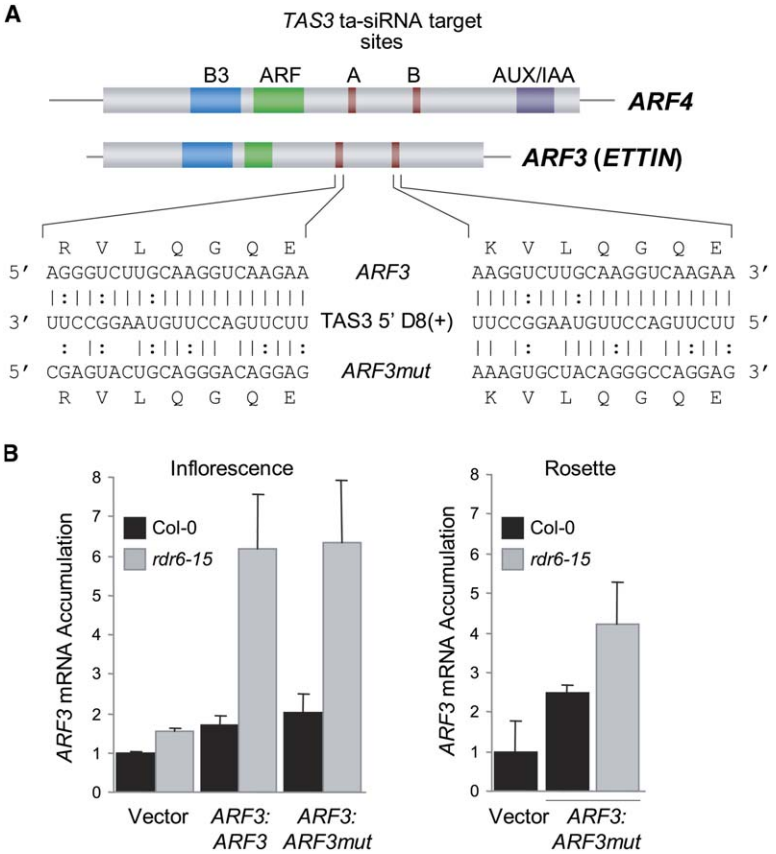

Figure 2. Expression of Targeted and Nontargeted *ARF3* Transgenes

(A) Domain organization of *ARF3* and *ARF4* mRNAs. The *TAS3* ta-siRNA target sites ("A" and "B" sites) in *ARF3*, and mutagenized sites in *ARF3mut*, are shown with base pairing to the *TAS3*-5′D8(+) ta-siRNA.

(B) Quantitative RT-PCR showing relative abundance of *ARF3* mRNA after normalization to *ACT2* mRNA (Col-0 vector-transformed level = 1.0). Standard errors of relative *ARF3* accumulation are shown. At left is the inflorescence tissue; at right is the rosette tissue.

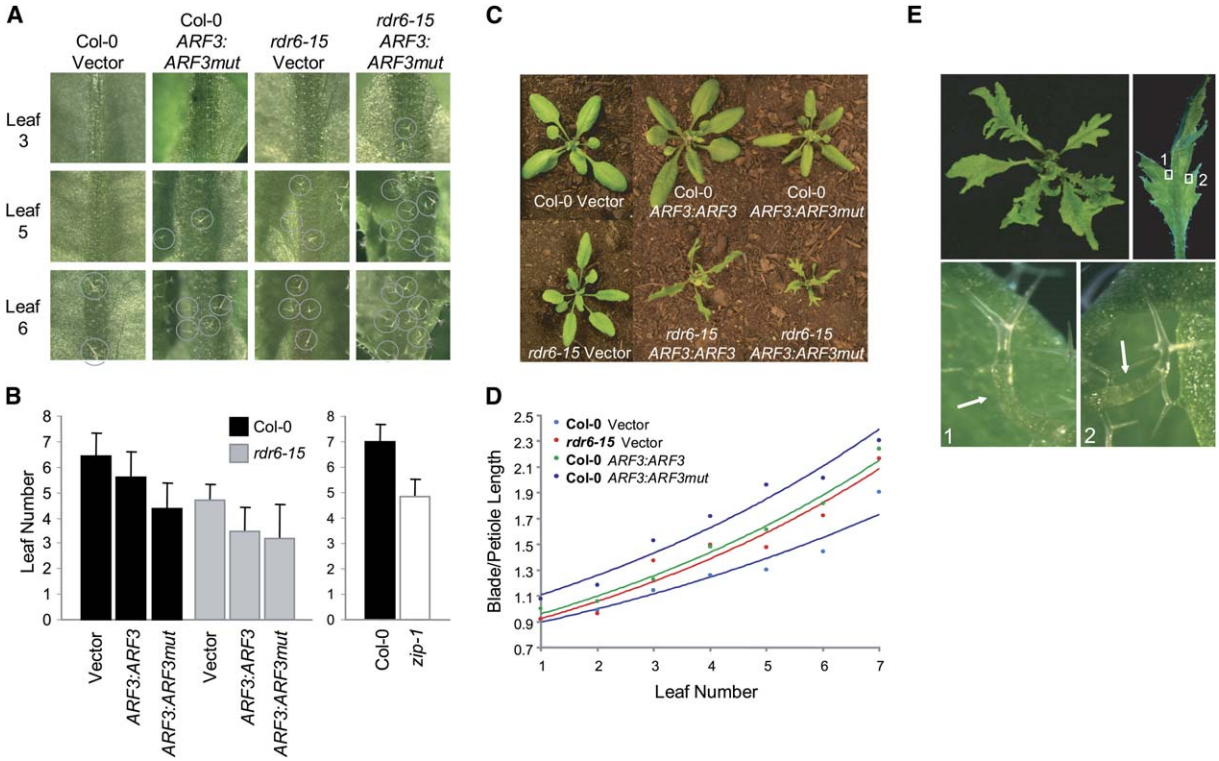

Figure 3. Accelerated-Phase-Change and Leaf-Morphology Phenotypes of Col-0 and *rdr6-15* Plants Expressing Either Targeted or Nontargeted *ARF3* Transgenes

(A) Abaxial surfaces of leaves 3, 5, and 6 in four plant lines as indicated above each column. Trichomes are circled.

(B) Mean leaf position at which abaxial trichomes were first detected. Standard errors of leaf position are shown. The two graphs show data for two independent experiments.

(C) Rosettes of 28-day-old plants.

(D) Ratio of leaf blade length/petiole length in leaves 1–7. Note that data are not shown for *rdr6-15* plants containing either transgene, because severe leaf distortion and lobing precluded accurate measurements.

(E) Rosette and cauline leaf of a *rdr6-15* plant containing the *ARF3:ARF3mut* transgene. The enlarged images show ectopic leaf primordia on abaxial surfaces (arrows).

in *rdr6-15* plants. *ARF3* levels in rosette tissue from Col-0 and *rdr6-15* plants containing the *ARF3:ARF3mut* transgene were also measured. As in inflorescence tissue, *ARF3* transcripts in *rdr6-15* transgenic plants accumulated to higher levels compared to those in Col-0 transgenic plants (Figure 2B). These data indicate that the sensitivity of *ARF3:ARF3mut* transgene mRNA to *TAS3* ta-siRNAs was decreased as a result of the mutations at the target sites.

The timing of first appearance of abaxial trichomes and of appearance of extended leaves, as well as leaf-curvature properties, were analyzed in 12–32 independent transformants of Col-0 and *rdr6-15* plants expressing empty vector, *ARF3:ARF3*, or *ARF3:ARF3mut* transgenes. In Col-0 plants, the nontargeted *ARF3:ARF3mut* transgene was predicted to confer dominant, accelerated phase-change phenotypes resembling those of *rdr6-15* and *zip-1* plants. The first abaxial trichomes in *rdr6-15* and *zip-1* plants appeared approximately two leaf positions ahead of abaxial trichomes in Col-0 (Figures 3A and 3B). Introduction of the *TAS3*-insensitive *ARF3:ARF3mut* transgene into Col-0 reproduced the precocious-abaxial-trichome phenotype to a level that was statistically indistinguishable from that in *rdr6-15* plants (p value = 0.23, permutation test) (Figure 3B). The *TAS3*-targeted *ARF3:ARF3* transgene in Col-0 resulted in an intermediate abaxial-trichome-timing phenotype that was only marginally different (p value = 0.052) from timing in Col-0 control plants (Figure 3B). In contrast, appearance of abaxial trichomes in *rdr6-15* plants expressing either *ARF3:ARF3* or *ARF3:ARF3mut* transgenes was accelerated significantly more than in Col-0 transgenic plants and was statistically distinguishable (p value < 0.002) from that in *rdr6-15* control plants (Figure 3B). These data indicate a correlation between *ARF3* expression levels resulting from derepression from *TAS3* and acceleration of abaxial trichomes.

The timing of appearance of extended or elongated leaf morphology during development was analyzed. Leaves emerging at or after position 3 in rosettes of ta-siRNA-deficient mutants (*rdr6-15*, *dcl4-2*, *zip-1*) were elongated compared to equivalent leaves in wild-type or control plants (Figures 1A and 3C). Col-0 plants containing the targeted *ARF3:ARF3* transgene had rosette leaves with an accelerated-elongation phenotype, with leaf blade length/petiole length ratios increasing at successive positions faster than in Col-0 plants (Figure 3D). These plants had blade/petiole ratios that were similar to those of *rdr6-15* plants at each position (Figure 3D). The timing of elongated leaves in Col-0 plants

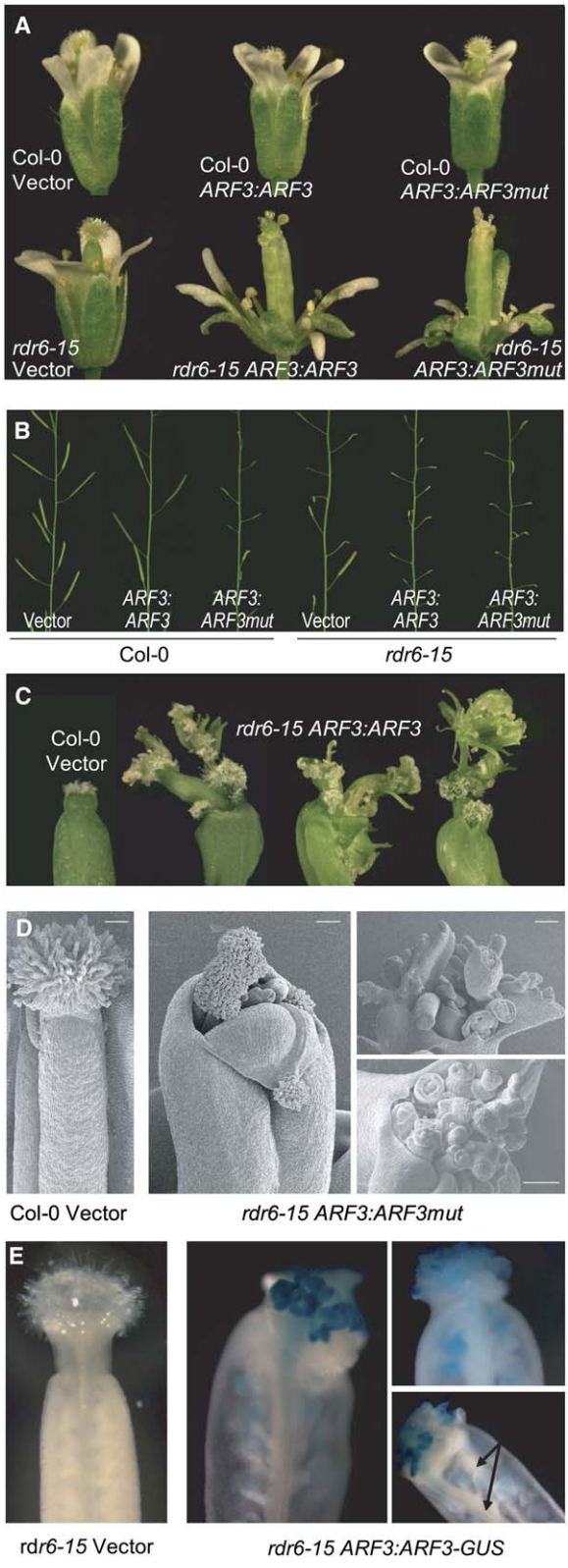

Figure 4. Flower Phenotypes of Col-0 and *rdr6-15* Plants Expressing *ARF3:ARF3* and *ARF3:ARF3mut* Transgenes

(A) Whole-flower phenotypes (stage 15).

(B) Siliques or nonfertile gynoecia.

(C) Apical zones of a stage 17+ flowers (Col-0 vector-transformed) or aberrant gynoecia in *rdr6-15* plants containing the *ARF3:ARF3* transgene.

Table 1. Effect of *ARF3* and *ARF3mut* Transgenes on Leaf Curvature and Shape

		Leaf Curvature[a]			
Genotype	n	None	Class 1	Class 2	Lobing
Col-0					
Vector	17	100.0	—	—	—
ARF3:ARF3	12	8.3	91.7	—	—
ARF3:ARF3mut	29	10.3	48.3	41.4	—
rdr6-15					
Vector	16	6.3	93.7	—	—
ARF3:ARF3	32	—	—	62.5	37.5
ARF3:ARF3mut	12	8.3	—	41.7	50.0

[a] Leaf-margin curvature and lobing are shown as a percentage of plants displaying phenotype. None, 0°–90° curvature; class 1, 90°–360° curvature; class 2, >360° curvature.

containing nontargeted *ARF3:ARF3mut* was also accelerated, but with exaggerated ratios at each position (Figure 3D). In plants with only moderate developmental abnormalities, both the *ARF3:ARF3* and *ARF3:ARF3mut* transgenes in *rdr6-15* plants conferred an enhanced elongated-leaf phenotype (data not shown). However, this was complicated by the high frequency of severe leaf-morphology defects in *rdr6-15* plants containing targeted and nontargeted constructs (Figure 3C), precluding measurements from most leaves.

The proportion of plants exhibiting downward curling of margins in rosette leaves was similar in *rdr6-15* control plants and Col-0 plants expressing either *ARF3:ARF3* or *ARF3:ARF3mut* transgenes (Table 1). In these three sets, at least 89% of plants had downward margin curvature of at least 90°. However, Col-0 plants containing *ARF3:ARF3mut* displayed a more severe curling phenotype, with over 41% of plants displaying at least 360° of curvature. In *rdr6-15* plants expressing either *ARF3:ARF3* or *ARF3:ARF3mut* transgenes, curvature when present was generally greater than 360°, again indicating that the effects of *ARF3* and *ARF3mut* expression were stronger in the *rdr6-15* background. A high proportion (37%–50%) of these plants also had severe leaf lobing (Table 1), stunting, and other patterning defects (see below).

These data show that characteristics typically associated with accelerated juvenile-to-adult phase change in ta-siRNA-deficient plants were reproduced (or enhanced) in Col-0 plants expressing the nontargeted *ARF3:ARF3mut* transgene and, to a limited extent, in plants expressing the targeted form. This supports the hypothesis that accelerated-timing defects of ta-siRNA-deficient mutants are due primarily to derepression of *ARF* gene targets of *TAS3* ta-siRNAs. The quantitatively weaker timing defect in Col-0 expressing the targeted *ARF3:ARF3* transgene, combined with the stronger defects in *rdr6-15* plants expressing either targeted or nontargeted transgenes, further suggests that

(D) Scanning electron microscopy (SEM) images of apical ends of gynoecia of stage 15 flowers from Col-0 vector-transformed or *rdr6-15 ARF3:ARF3mut*-transformed plants.

(E) GUS activity in gynoecia of *rdr6-15* plants transformed with either empty vector (left) or *ARF3:ARF3-GUS* transgene (right). Arrows point to a split septum.

the phase-change phenotype is *ARF3* dosage dependent. As dosage progressively increases in different lines—by addition of *ARF3* copies, derepression of endogenous or transgenic copies, or copy-number addition plus derepression—phase-change timing is progressively accelerated. A role for *ARF3*, and potentially other *ARFs* with *TAS3* ta-siRNA target sites, in developmental timing suggests a key role for auxin signaling in the juvenile-to-adult phase transition.

Targeted and Nontargeted *ARF3* Transgenes in *rdr6-15* Cause Patterning Defects

The timing defects in *rdr6-15* plants and Col-0 plants containing the nontargeted *ARF3:ARF3mut* transgene were accompanied by additional phenotypes in reproductive organs, including reduced seed set as shown previously for *rdr6* mutants [4]. Combining the *ARF3:ARF3* or *ARF3:ARF3mut* transgenes with the *rdr6-15* mutation, however, resulted in severe vegetative and reproductive phenotypes. In rosettes, leaves were narrow, highly twisted and curled, and irregularly shaped (Figures 3C and 3E). In the most severely affected plants, leaves were deeply lobed. Lobed leaves contained ectopic radial leaf primordia that emerged either from the margin of the petiole near the base of the leaf or from the tips of veins near the sinuses of the lobes on the abaxial surface (Figure 3E). The lobing and ectopic leaf primordia were reminiscent of plants that overexpress class I *KNOTTED1*-like homeobox (*KNOX*) genes [20] and of *asymmetric leaves2* (*as2*) *rdr6* double mutants, which contain abaxialized leaves [21]. These phenotypes were not detected in *rdr6* mutants alone, indicating that derepression and overexpression of *ARF3* triggers these effects. These data suggest that *ARF3* may positively regulate *KNOX* genes, perhaps through negative regulation of *AS1/AS2* [22–24]. This scenario specifies *TAS3* ta-siRNAs as negative regulators of abaxial cell fate through suppression of *ARF3* and, likely, *ARF4*.

Developing flowers of *rdr6-15* plants expressing either *ARF3:ARF3* or *ARF3:ARF3mut* transgenes had many severe defects. Sepals and petals were downwardly curled, narrow, and twisted and failed to enclose the inner organs (Figure 4A). Stamens were short with anthers lacking pollen, and gynoecia were irregular in shape, swollen, and frequently split or open at the apical end (Figure 4A). These flowers were sterile, although gynoecia continued to expand to resemble short, wide siliques with unfertilized ovules (Figures 4A and 4B). Valve tissue at the apical end was often folded back on itself, with little or no style tissue and irregular patches of stigmatic tissue (Figure 4D). Ectopic gynoecia, ovules, filaments, and disorganized growths, some with stigmatic tissue, emerged from open gynoecia (Figures 4C and 4D). The ectopic organs initiated from the placentas, filling the apices of the gynoecia, and accounted for the swollen and irregular shapes. These organs continued to grow past stage 17 when wild-type flowers were developing into siliques. *rdr6-15* plants were transformed with *ARF3:ARF3-GUS* and *ARF3:ARF3mut-GUS* transgenes containing β-glucuronidase (GUS) translationally fused to *ARF3* and *ARF3mut* coding sequences to determine whether *ARF3* expression was associated with these ectopic organs. In all flowers with a severe phenotype and containing either transgene, GUS activity was detected in the ovules and the ectopic growths, indicating that *ARF3* was highly expressed in the proliferating tissues of these flowers (Figure 4E).

Severely affected gynoecia also had split septa that were occasionally still fused at the basal end (Figure 4E). Mutants of *TOUSLED* (*TSL*), *LEUNIG* (*LUG*), *AINTEGUMENTA* (*ANT*), *SPATULA* (*SPT*), and *CRABS CLAW* (*CRC*) also have split septa and carpels [25–27]. Genetic data indicate that *ARF3* represses or restricts the expression of both *TSL* and *SPT* [27, 28], suggesting that the gynoecium phenotypes observed in *rdr6-15* plants containing *ARF3:ARF3* or *ARF3:ARF3mut* could be due to spatial or temporal repression of *TSL* and *SPT* and possibly to other flower patterning factors. Ta-siRNA-defective mutants also form carpels with a split septum that produces stigmatic tissue at the apical end [4], although to a lesser extent than that observed in *rdr6-15* plants containing *ARF3:ARF3* or *ARF3:ARF3mut*. Loss of septum and transmitting-tract tissue may indicate abaxialization, or loss of adaxial tissues, in carpels.

It is not clear how *ARF3* activity, as well as regulation of *ARF3* by *TAS3* ta-siRNAs, affects both vegetative timing and polarity of lateral organs. It is possible that timing of the juvenile-to-adult transition is merely a consequence of subtle, *TAS3* ta-siRNA-mediated changes in adaxial/abaxial polarity factors to an extent that does not dramatically affect establishment of organ asymmetry. Alternatively, differential regulation of *ARF3* by *TAS3* ta-siRNAs at different times or in different domains during primordia development may result in two different outputs.

Supplemental Data

Supplemental Data include Supplemental Experimental Procedures and are available with this article online at: http://www.current-biology.com/cgi/content/full/16/9/939/DC1/.

Acknowledgments

We thank Al Soeldner and Teresa Sawyer for scanning electron microscopy, Heather Sweet for excellent plant management and care, Bobby Babra for help with RNA blot assays, Kristin Kasschau for advice on microscopy, Scott Poethig for *zip-1* seed, and Detlef Weigel for helpful discussions. This work was supported by grants from National Science Foundation Grant MCB-0209836, National Institutes of Health Grant AI43288, and U.S. Department of Agriculture Grant 2005-35319-15280.

Received: February 15, 2006
Revised: March 12, 2006
Accepted: March 21, 2006
Published: May 8, 2006

References

1. Allen, E., Xie, Z., Gustafson, A.M., and Carrington, J.C. (2005). microRNA-directed phasing during trans-acting siRNA biogenesis in plants. Cell *121*, 207–221.
2. Gasciolli, V., Mallory, A.C., Bartel, D.P., and Vaucheret, H. (2005). Partially redundant functions of *Arabidopsis* DICER-like enzymes and a role for DCL4 in producing trans-acting siRNAs. Curr. Biol. *15*, 1494–1500.
3. Jones-Rhoades, M.W., Bartel, D.P., and Bartel, B. (2006). MicroRNAs and their regulatory roles in plants. Annu. Rev. Plant Biol. *57*, 19–53.
4. Peragine, A., Yoshikawa, M., Wu, G., Albrecht, H.L., and Poethig, R.S. (2004). SGS3 and SGS2/SDE1/RDR6 are required for

juvenile development and the production of trans-acting siRNAs in *Arabidopsis*. Genes Dev. *18*, 2368–2379.
5. Vazquez, F., Vaucheret, H., Rajagopalan, R., Lepers, C., Gasciolli, V., Mallory, A.C., Hilbert, J.L., Bartel, D.P., and Crete, P. (2004). Endogenous trans-acting siRNAs regulate the accumulation of *Arabidopsis* mRNAs. Mol. Cell *16*, 69–79.
6. Xie, Z., Allen, E., Wilken, A., and Carrington, J.C. (2005). DICER-LIKE 4 functions in trans-acting small interfering RNA biogenesis and vegetative phase change in *Arabidopsis thaliana*. Proc. Natl. Acad. Sci. USA *102*, 12984–12989.
7. Yoshikawa, M., Peragine, A., Park, M.Y., and Poethig, R.S. (2005). A pathway for the biogenesis of trans-acting siRNAs in *Arabidopsis*. Genes Dev. *19*, 2164–2175.
8. Williams, L., Carles, C.C., Osmont, K.S., and Fletcher, J.C. (2005). A database analysis method identifies an endogenous trans-acting short-interfering RNA that targets the *Arabidopsis ARF2, ARF3*, and *ARF4* genes. Proc. Natl. Acad. Sci. USA *102*, 9703–9708.
9. Hunter, C., Sun, H., and Poethig, R.S. (2003). The *Arabidopsis* heterochronic gene *ZIPPY* is an ARGONAUTE family member. Curr. Biol. *13*, 1734–1739.
10. Willmann, M.R., and Poethig, R.S. (2005). Time to grow up: The temporal role of small RNAs in plants. Curr. Opin. Plant Biol. *8*, 548–552.
11. Vaucheret, H., Vazquez, F., Crete, P., and Bartel, D.P. (2004). The action of ARGONAUTE1 in the miRNA pathway and its regulation by the miRNA pathway are crucial for plant development. Genes Dev. *18*, 1187–1197.
12. Zilberman, D., Cao, X., and Jacobsen, S.E. (2003). ARGONAUTE4 control of locus-specific siRNA accumulation and DNA and histone methylation. Science *299*, 716–719.
13. Zilberman, D., Cao, X., Johansen, L.K., Xie, Z., Carrington, J.C., and Jacobsen, S.E. (2004). Role of *Arabidopsis* ARGONAUTE4 in RNA-directed DNA methylation triggered by inverted repeats. Curr. Biol. *14*, 1214–1220.
14. Baumberger, N., and Baulcombe, D.C. (2005). *Arabidopsis* ARGONAUTE1 is an RNA slicer that selectively recruits microRNAs and short interfering RNAs. Proc. Natl. Acad. Sci. USA *102*, 11928–11933.
15. Pekker, I., Alvarez, J.P., and Eshed, Y. (2005). Auxin response factors mediate *Arabidopsis* organ asymmetry via modulation of *KANADI* activity. Plant Cell *17*, 2899–2910.
16. Hagen, G., and Guilfoyle, T. (2002). Auxin-responsive gene expression: Genes, promoters and regulatory factors. Plant Mol. Biol. *49*, 373–385.
17. Tiwari, S.B., Hagen, G., and Guilfoyle, T. (2003). The roles of auxin response factor domains in auxin-responsive transcription. Plant Cell *15*, 533–543.
18. Jones-Rhoades, M.W., and Bartel, D.P. (2004). Computational identification of plant microRNAs and their targets, including a stress-induced miRNA. Mol. Cell *14*, 787–799.
19. Schwab, R., Palatnik, J.F., Riester, M., Schommer, C., Schmid, M., and Weigel, D. (2005). Specific effects of microRNAs on the plant transcriptome. Dev. Cell *8*, 517–527.
20. Ori, N., Eshed, Y., Chuck, G., Bowman, J., and Hake, S. (2000). Mechanisms that control *knox* gene expression in the *Arabidopsis* shoot. Development *127*, 5523–5532.
21. Li, H., Xu, L., Wang, H., Yuan, Z., Cao, X., Yang, Z., Zhang, D., Xu, Y., and Huang, H. (2005). The putative RNA-dependent RNA polymerase RDR6 acts synergistically with ASYMMETRIC LEAVES1 and 2 to repress BREVIPEDICELLUS and microRNA165/166 in *Arabidopsis* leaf development. Plant Cell *17*, 2157–2171.
22. Byrne, M.E., Barley, R., Curtis, M., Arroyo, J.M., Dunham, M., Hudson, A., and Martienssen, R.A. (2000). Asymmetric leaves1 mediates leaf patterning and stem cell function in *Arabidopsis*. Nature *408*, 967–971.
23. Semiarti, E., Ueno, Y., Tsukaya, H., Iwakawa, H., Machida, C., and Machida, Y. (2001). The *ASYMMETRIC LEAVES2* gene of *Arabidopsis thaliana* regulates formation of a symmetric lamina, establishment of venation and repression of meristem-related homeobox genes in leaves. Development *128*, 1771–1783.
24. Xu, L., Xu, Y., Dong, A., Sun, Y., Pi, L., Xu, Y., and Huang, H. (2003). Novel *as1* and *as2* defects in leaf adaxial-abaxial polarity reveal the requirement for ASYMMETRIC LEAVES1 and 2 and ERECTA functions in specifying leaf adaxial identity. Development *130*, 4097–4107.
25. Alvarez, J., and Smyth, D.R. (1999). *CRABS CLAW* and *SPATULA*, two *Arabidopsis* genes that control carpel development in parallel with *AGAMOUS*. Development *126*, 2377–2386.
26. Liu, Z., Franks, R.G., and Klink, V.P. (2000). Regulation of gynoecium marginal tissue formation by LEUNIG and AINTEGUMENTA. Plant Cell *12*, 1879–1892.
27. Roe, J.L., Nemhauser, J.L., and Zambryski, P.C. (1997). TOUSLED participates in apical tissue formation during gynoecium development in *Arabidopsis*. Plant Cell *9*, 335–353.
28. Heisler, M.G., Atkinson, A., Bylstra, Y.H., Walsh, R., and Smyth, D.R. (2001). *SPATULA*, a gene that controls development of carpel margin tissues in *Arabidopsis*, encodes a bHLH protein. Development *128*, 1089–1098.